ГОДИШНИК НА УНИВЕРСИТЕТА ПО АРХИТЕКТУРА, СТРОИТЕЛСТВО И ГЕОДЕЗИЯ СОФИЯ

Том Volume 56 2023 Брой Issue 3

ANNUAL OF THE UNIVERSITY OF ARCHITECTURE, CIVIL ENGINEERING AND GEODESY SOFIA

Received: 09.12.2022 г.
Accepted: 21.12.2022 г.

DETERMINATION OF AERODYNAMIC COEFFICIENTS UNDER WIND LOADS ON BEAM BRIDGES

L. Zdravkov[1]

Keywords: *wind, load, bridge, longitudinal beam, aerodynamic coefficient, CFD analysis*

ABSTRACT

The wind often is the authoritative horizontal load in the transverse direction for bridges. For this reason, special attention has been paid to them in wind load standards. Unfortunately, all available load standards indicate one, summarized value for aerodynamic coefficient. It corresponds to the entire section of the facility. There is no division on the individual beams and / or the roadway. Information about the specific wind pressure on each of the beams is needed for the correct design of the supporting systems. To fill this gap, the author has created multiple models of bridges with longitudinal beams, using a computerized fluid simulation (CFD) program. According to the basic idea, there are no vehicles on the bridges. However, in order to expand the representativeness of the study, vehicles were placed on the bridges. Using these computer models, the author determined the values of the static aerodynamic coefficients for each of the bridge beams under the roadway and for the cross section of the bridge as a whole. The results clearly show that the values of the aerodynamic coefficients for the entire section of the bridge are much lower than those accounted for the windward beam.

1. Introduction

Bridges are building facilities that are operated outdoors. Often the wind is the leading horizontal effect in a crosswise direction. Therefore, in the standards for loads on bridges such AS/NZS 1170.2:2011 [1], BS 5400-2:2006 [2], EN 1991-1-4:2005 [3], IRC: 6-2017:2017 [4], Ordinance for the design of road and railway bridges and culverts of 1989 [5] and CP 35.13330.2011 [6], on the wind effect is given due attention. To increase safety, the values of the

[1] Lyubomir Zdravkov, Assoc. Prof. Dr. Eng., Dept. “Steel, Timber and Plastic Structures”, UACEG, 1 H. Smirnenski Blvd., Sofia 1046, e-mail: zdravkov_fce@uacg.bg

aerodynamic coefficients specified in these standards are increased several times compared to these for buildings. Unfortunately, the presented in the documents above aerodynamic coefficients, refer to the entire cross-section of the bridge structure. There is no separation and additional information by elements. Only BS 5400-2:2006 [2] states that the aerodynamic coefficient for composite beams is 2.2, without accounting for any shielding. An information about the wind load on each of the beams is necessary for the correct design of their supporting systems. One possible approach is to determine the aerodynamic coefficient for the entire cross-section of the bridge and apply it separately to each of its elements. Another possible solution is to look for some analogy with known facilities. But do any of these approaches produce reliable results? In order to answer these questions, through a computer fluid simulation (CFD) program, the author has built and studied numerous models of girder bridges. Through them, he determined the values of the static aerodynamic coefficients for each longitudinal beam under the road plate and for the bridge section as a whole.

2. Model description

Computational Fluid Dynamics (CFD) analysis is selected as a suitable approach to be used in the present study. Through the graphical interface Workbench of ANSYS [7] and its module Fluid Flow (CFX) have been created two general spatial models of bridge structures. In the first model the girders are with a rectangular cross section, by reinforced concrete. In the second model the girders are made of steel sheets. The height of all beams is 1,000 mm. The reinforced concrete beams are 400 mm wide, the steel ones - as is shown in fig. 1*b*. Reinforced concrete slab with a thickness of 200 mm is placed above the girders there, see fig. 1.

To increase the scope and usefulness of the study, the following submodels have been created:

a) the number of beams under the slab n = 2, 3 and 4;

b) the distance between the beams x = 1, 2, 3, 4 and 5 m.

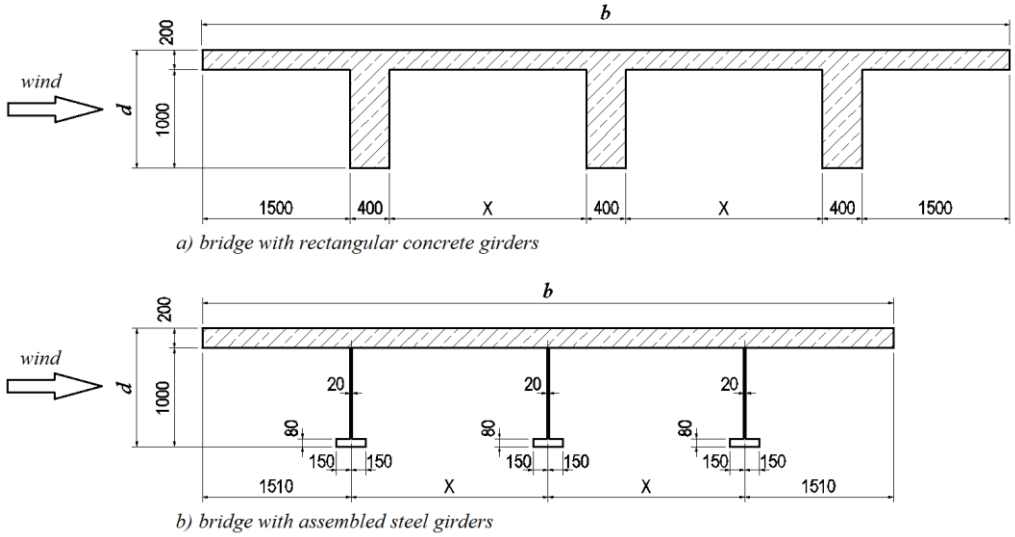

Fig. 1. Cross-section of researched bridges

A spatial analysis is used in this paper. A typical cross-section of the bridge's structure is modelled in 2D and then extruded into a 6 m depth making an overall domain shape of a parallelepiped. Around the bridge structures are created box enclosure, see fig. 3. The walls of the simulated wind tunnel around each bridge section are located at the following distances from them:

a) for bridges with two or three girders:

- fluid inlet - 5 m;
- fluid outlet - at 20 m, i.e. the body of the bridge is located much closer to the inlet of the wind tunnel, see fig. 2;
- vertical sidewalls - as the "Symmetry" option is used, there is no distance between the walls and the cross-section of the bridge;
- horizontal walls (bottom and roof) - 10 m.

b) for bridges with four girders:

- fluid inlet - at 8 m;
- fluid outlet - at 32 m;
- vertical sidewalls - as the "Symmetry" option is used, there is no distance between them and the cross-section of the bridge;
- horizontal walls (bottom and roof) - 16 m.

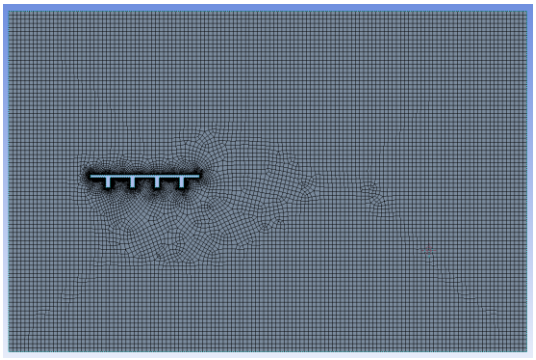

Fig. 2. Refinement of the mesh around the bridge elements

The determining of the above-written distances between the walls of the virtual wind tunnel and bridge is based on the principle that airflow adjacent to the bridge should not affected, see *Rusev et al.* [8]. Accepted distances are bigger than requirements of *Tominaga et al.* [9], as follow:

- the top / bottom boundary should be set 5H or more away the obstacle, where H is the height of the bridge section in the current research ($H = d$ = 1,200 mm, see fig.1);
- the outflow boundary should be set at least 10H behind the obstacle.

At the same time, to avoid heavy computer solutions and save computational time, the maximum number of finite elements is maintained into reasonable limits. To optimize their mesh, it is significantly refined in the area around the bridge, see fig. 2, and is sparse to the periphery, as is done in *Rusev et al.* [10]. The maximum size of the finite elements of the air is limited to:

a) elements in direct contact with the slab and girders – 20 mm;

b) all other elements – 400 mm.

The “Quadratic” option is used when creating the mesh of finite elements, as a result of which the nodes in the middle of their sides are preserved. This type of element is characterized by its nonlinear deformation behaviour.

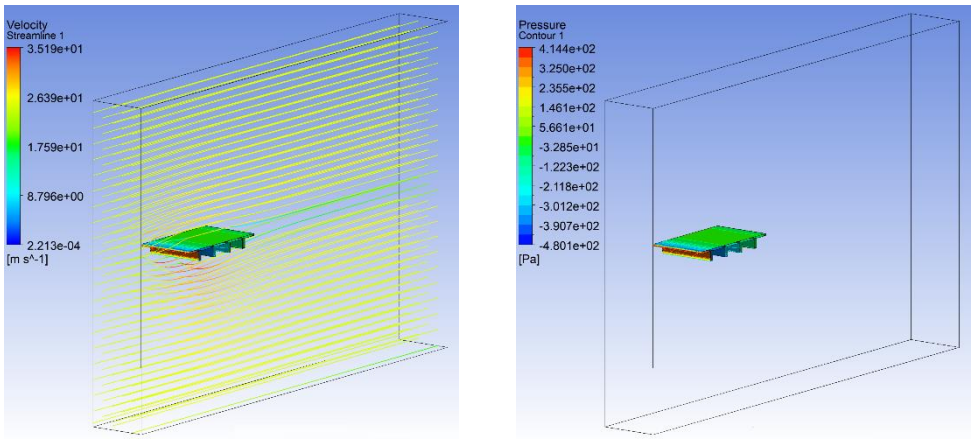

a) velocity of the wind flow around the bridge *b) pressure on surfaces of the bridge elements*

Fig. 3. Wind flow around the bridge and the resulting pressure on the elements

Steady state analysis type is used in a Fluid flow (CFX) module. K-ε model, part of *Reynolds-averaged Navier Stokes* (RANS) family, is used to simulate the turbulent flow of the fluid around the bridges. They look like as [11]:

$$\frac{\partial \overline{u_i}}{\partial t} + \frac{\partial \left(\overline{u_i}\,\overline{u_j} \right)}{\partial x_j} = -\frac{1}{\rho}\frac{\partial \overline{p}}{\partial x_i} + \nu \frac{\partial^2 \overline{u_i}}{\partial^2 x_j} - \frac{\partial \left(\overline{u_i'}\,\overline{u_j'} \right)}{\partial x_j}, \tag{1}$$

where $\overline{u_i}$ is the mean speed of the fluid;

$\overline{u_i'}$ – the change of the speed;

ρ – the density of the fluid;

v – the cinematic viscosity;

t – the time;

$\overline{p}$ – the pressure of the fluid;

$\overline{u_i'}\,\overline{u_j'} = \tau_{ij}$ – tensor of the stresses of *Reynolds*

In analogy to molecular viscous stresses, Reynolds stresses can be represented as [12]:

$$\tau_{ij} = \overline{u_i'}\,\overline{u_j'} = \frac{2}{3}k\delta_{ij} - \nu_t \left(\frac{\partial \overline{u_i}}{\partial x_j} + \frac{\partial \overline{u_j}}{\partial x_i} \right), \tag{2}$$

where k is the kinetic turbulence energy;

$\nu_t = \mu_t/\rho$ – turbulence or eddy (kinematic) viscosity.

In the models with one equation v_t is accounted by the expression [11]:

$$\nu_t = C_{\nu 1}\sqrt{kL}\,, \tag{3}$$

in which $C_{\nu 1}$ is dimensionless parameter.

A two-equation model, such as the used here standard k–ε model, uses differential equations to calculate the characteristic velocity, on the length scale L, and then evaluates the value of ν_t by the following equation [13]:

$$\nu_t = C_\mu \frac{k^2}{\varepsilon}\,, \tag{4}$$

where C_μ = 0,09;

ε – the turbulence dissipation rate.

These RANS equations are an adequate representation of the wind tunnel's reality, *Baklanov et al.* [14] Accepted turbulence has a medium (5%) intensity. No combustion and thermal radiation. The used fluid is an air ideal gas with a temperature of 25 °C. Its speed at the inlet domain of the tunnel is constant in height and has a value of v = 25 m/s. Flow regimes in outlet and opening domains are subsonic, with a relative pressure 0 Pa. Flow direction is normal to boundary conditions. Bridge section domain is no slip rough wall. The models of the bridge with rectangular reinforced concrete beams, see fig. 1*a*, have roughness with a high of 0.5 mm on all surfaces. Models with steel girders, see fig. 1*b*, have roughness with a height of 0.1 mm on all surfaces. The surface of the terrain under the bridge is perfectly smooth.

Unlike of the research of *Mei Yu et al.* [15], there main wind flow is horizontal, i.e. the angle of attack is 0°. The direction of the approaching wind is perpendicular to the longitudinal axes of the bridge girders and deck.

During its movement, the wind flows around the bridge, see fig. 3*a*, which leads to the appearance of pressure on its elements, see fig. 3*b*. As a result, generated in the bridge girders forces could be accounted for. Knowing the value of forces and area of the girders, the value of the total (whole) wind pressure on the girders can be determined by the formula:

$$q_{cp,x} = \frac{F_{x,i}}{A_g}\,, \tag{5}$$

where $q_{cp,x}$ is the total (whole) pressure on the i-th bridge girder. It is equal to the sum of the conditionally positive (compression) and negative (suction) pressure on the girder;

$F_{x,i}$ – the value of the accounted force on the i-th girder in the direction of the horizontal wind flow;

A_g – the area of the i-th girder, transverse to the wind flow.

Reference mean (basic) velocity pressure q_b could be determined by the written in EN 1991-1-4:2005 formula:

$$q_b = \frac{1}{2}\rho v_b^2 = \frac{1}{2}1.25\cdot 25^2 = 390\ \text{N/m}^2\,, \tag{6}$$

where ρ = 1.25 kg/m^3 is the air density;

v_b = 25 m/s – accepted wind speed in the current research.

The ratio of the total pressure $q_{cp,x}$ on the girders and the reference mean pressure q_b give us information about the value of the total aerodynamic coefficient $C_{cp,x}$ of the girders, i.e.:

$$C_{cp,x} = \frac{q_{cp,x}}{q_b}. \tag{7}$$

To account for the influence on the wind load due to a vehicle on the bridge, a vehicle is simulated in the rectangular reinforced concrete beam model. Its dimensions and location are shown in fig. 4. All other parameters are as already described above.

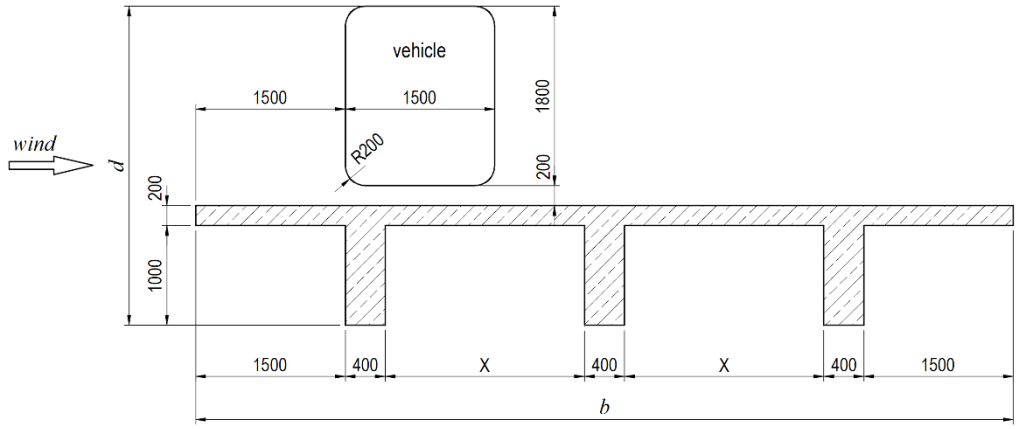

Fig. 4. Concrete bridge with a vehicle on it – position and dimensions

3. Results

The values of the aerodynamic coefficients $C_{cp,x}$ for wind load in the horizontal plane on bridges without vehicle on it, obtained by equations (5-7), are shown in fig. 5, where:

x is the "clear" distance between the rectangular girders, see fig. 1*a*;

b – the entire width of the bridge section;

d = 1.2 m – the entire height of the cross-section of the bridge;

$C_{cp,x,L}$ – the total aerodynamic coefficient for the windward (left in this case) girder;

$C_{cp,x,R}$ – the total aerodynamic coefficient for the leeward (right here) girder;

$C_{cp,x,tot}$ – the total aerodynamic coefficient for the whole section of the bridge;

$C_{cp,x,m}$ – the total aerodynamic coefficient for the middle girder;

$C_{cp,x,m,L}$ – the total aerodynamic coefficient for the left internal girder, in the direction of the wind flow;

$C_{cp,x,m,R}$ – the total aerodynamic coefficient for the right internal girder.

When the value of the aerodynamic coefficient $C_{cp,x}$ is positive, it means that the equivalent force $F_{x,i}$ on the corresponding girder has the same direction of action as the wind flow. When $C_{cp,x}$ has a negative value, it means that the equivalent force $F_{x,i}$ has a direction of action opposite to the wind flow.

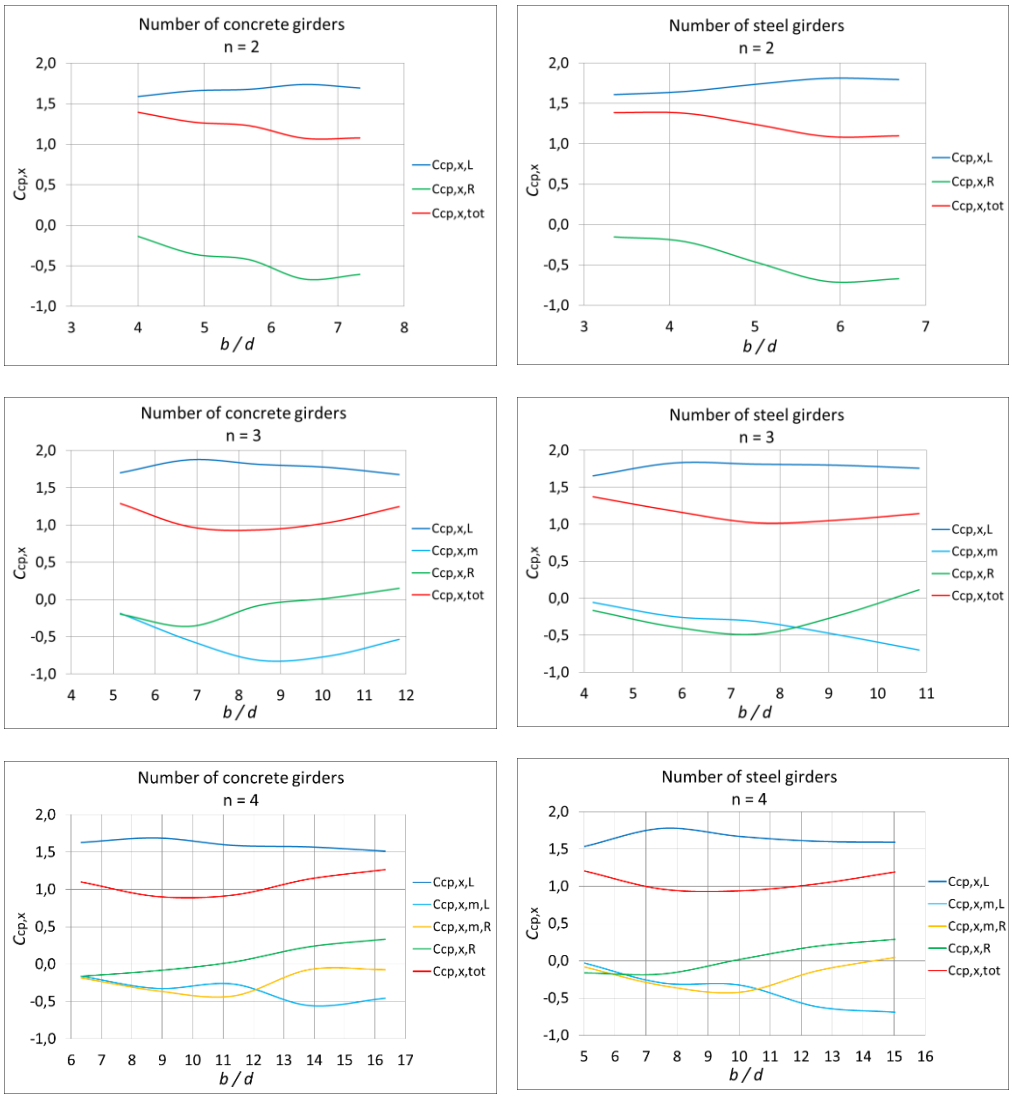

a) rectangular concrete girders *b) steel girders*

Fig. 5. Values of the coefficient $C_{cp,x}$ for bridges without vehicles on it

Here is interesting that the equivalent force on the windward beam (the left in these models) always has a direction coinciding with that of the wind flow. As a result, only positive values of the aerodynamic coefficient were recorded, which are within the limits $C_{cp,x,L} = 1.51 \div 1.88$. They are smaller than shown in BS 5400-2:2006 value of the coefficient $C_{cp,x} = 2.2$, but are greater than the *Wassef* [16] value of $C_{cp,x} = 1.3$.

The equivalent force on the leeward (right in this case) girder can have a direction that is coincides with or is opposite to that of the wind flow. The accounted values of the aerodynamic coefficient are within the limits $C_{cp,x,R} = -0.71 \div 0.33$.

The forces on the internal girders always are in opposite direction to the wind flow. The accounted values of the aerodynamic coefficient are $C_{cp,x,m}$ = -0.82 ÷ 0.

The accounted values of the aerodynamic coefficient for the entire section of the bridge are positive only and are within the limits $C_{cp,x,tot}$ = 0.9 ÷ 1.39, i.e. they are smaller than those accounted for the windward beam.

The vertical force $F_{z,tot}$, which acts on the entire section of the bridge, also was taken into account. Using formulas (5-7), adapted for the vertical projection of the bridge, the values of the total aerodynamic coefficients $C_{cp,z,tot}$ were determined for the wind load in the vertical plane for the entire section of the bridge. They are shown graphically in fig. 6.

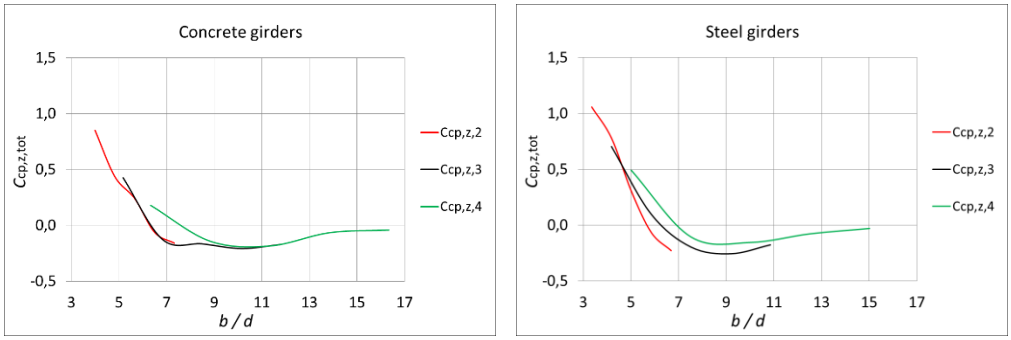

a) rectangular concrete girders *b) steel girders*

Fig. 6. Values of the coefficient $C_{cp,z,tot}$ for bridges without vehicles on it

The shown in fig. 5 and fig. 6 values of the aerodynamic coefficients for bridges without a vehicle on them slightly differ from these obtained in a previous study by the author [17]. This is due to the different mesh density of the finite elements that are in direct contact with the bridge surfaces. They are smaller here, with a maximum size of 20 mm, i.e. the net is denser.

When the value of the aerodynamic coefficient $C_{cp,z,tot}$ is positive, it means that the equivalent force $F_{z,total}$ on the bridge has a direction of action from the bottom up. When $C_{cp,z,tot}$ has a negative value, it means that the equivalent force $F_{z,total}$ has a direction of action from top to bottom, i.e. coinciding with gravity.

Here it is striking that for small values of the b/d ratio, the equivalent vertical force $F_{z,total}$ acts from the bottom up. The accounted maximum value of the total aerodynamic coefficient is $C_{cp,z,tot}$ = 1.06. At larger values of the b/d ratio, the equivalent vertical force $F_{z,total}$ acts from top to bottom, i.e. wind loads have the same direction as gravity loads. Values of the total aerodynamic coefficient of the order of $C_{cp,z,tot}$ = -0.26 are accounted here. It can be seen that there is a difference with the value $C_{cp,z,tot}$ = ±0.9 recommended in EN 1991-1-4:2005 [3].

The wind flow around the bridge with a vehicle on it is shown in fig. 7*a*, and the resulting pressure on its surfaces - in fig. 7*b*.

The values of the aerodynamic coefficients $C_{cp,x}$ for wind loading on a bridge with a vehicle on it are shown in fig. 8.

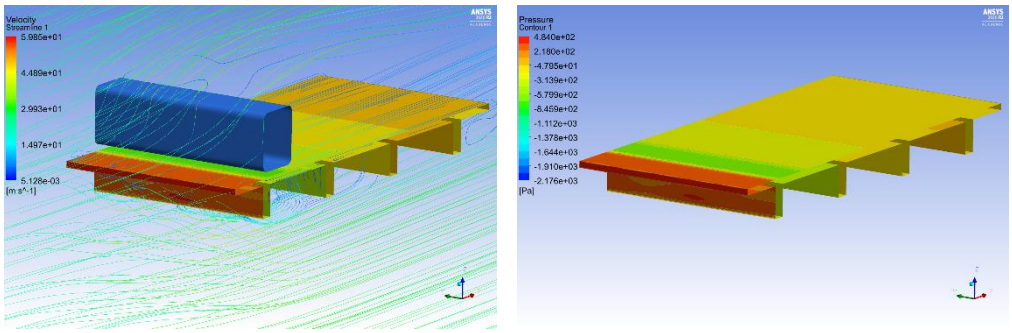

a) velocity of the wind flow around the bridge *b) pressure on surfaces of the bridge elements*

Fig. 7. Wind flow around the bridge with a vehicle on it and the resulting pressure on the elements

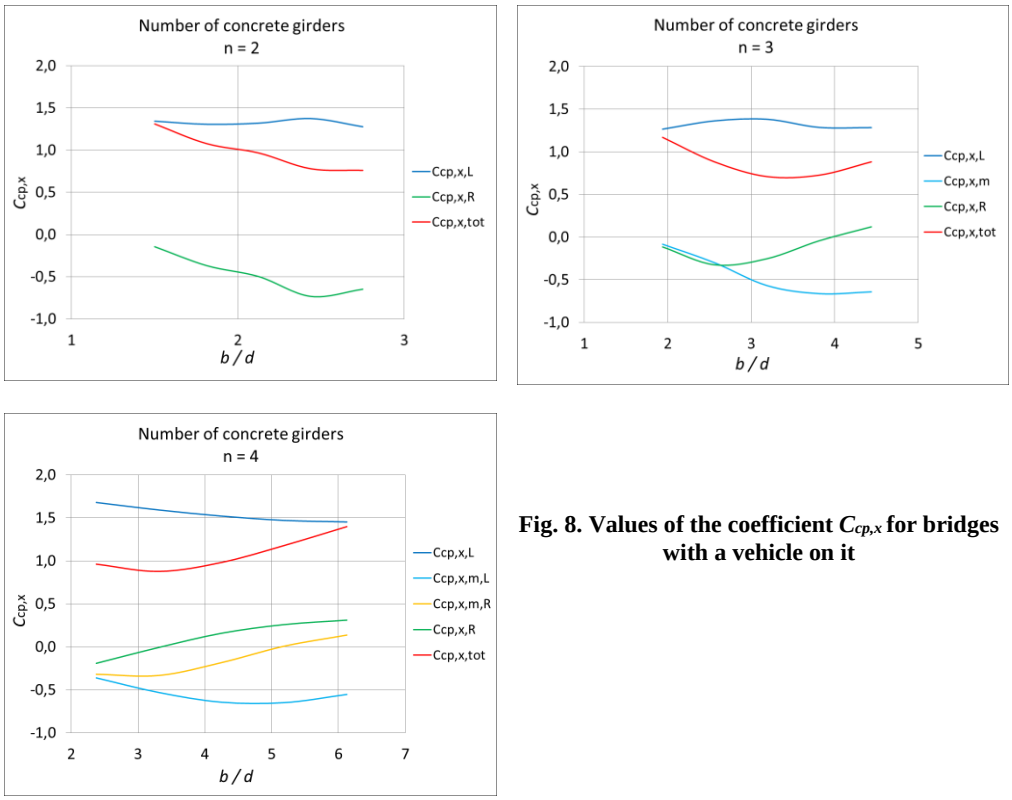

Fig. 8. Values of the coefficient $C_{cp,x}$ for bridges with a vehicle on it

Here again is interesting that the equivalent force on the windward (left in these models) beam always has a direction coinciding with that of the wind flow. As a result, only positive values of the aerodynamic coefficient were recorded, which are within the limits $C_{cp,x,L} = 1.27 \div 1.68$. They are smaller than the shown above values for $C_{cp,x,L}$ when blowing a bridge without a vehicle on it. The equivalent force on the leeward (right in this case) girder can have a direction

that is coincides with or is opposite to that of the wind flow. The values of the aerodynamic coefficient recorded here are within the limits $C_{cp,x,R}$ = -0.73 ÷ 0.31.

The forces on the internal beams are in a direction that coincides to or is opposite to that of the wind flow. The accounted values of the aerodynamic coefficient are $C_{cp,x,m}$ = -0.66 ÷ 0.137.

The accounted values of the aerodynamic coefficient for the whole section of the bridge are positive only and are within the limits $C_{cp,x,tot}$ = 0.71 ÷ 1.4, i.e. they are smaller than these accounted for the windward girder.

The vertical force $F_{z,tot}$, which acts on the entire section of the bridge, was also taken into account in the current research. Using formulas (5-7), adapted for the vertical projection of the bridge, were determined the values of the total aerodynamic coefficients $C_{cp,z,tot}$ for the wind load in the vertical plane for the entire section of the bridge. They are shown graphically in Fig. 9. The accounted values of the total aerodynamic coefficient are within the limits $C_{cp,z,tot}$ = -0.31 ÷ 0.34.

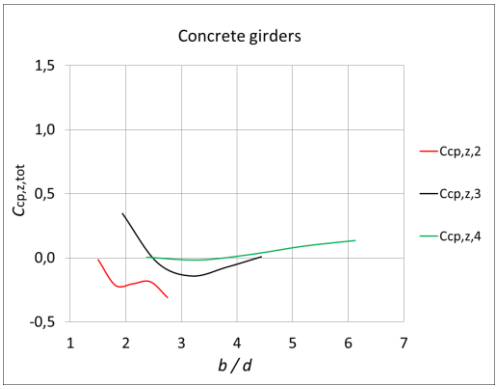

Fig. 9. Values of the coefficient $C_{cp,z,tot}$ for bridges with a vehicle on it

3. Conclusions

In widespread standards for loading on bridges does not exist information about wind loading on the individual elements. For their determination, through the graphical interface Workbench of ANSYS (2020) and its module for computational fluid dynamics Fluid Flow (CFX) are researched several typical bridge sections with longitudinal girders. The following conclusions could be drawn from the conducted study:

a) the windward beams are the heaviest loaded by the wind flow;

b) the total load on the leeward girders may have a direction that coincides with or is opposite to that of the wind flow. The reference aerodynamic coefficients are two to three times smaller than those for the windward girders;

c) the total load on the internal girders is always in the opposite direction to the wind flow;

d) the accounted values of the aerodynamic coefficient for the whole section of the bridges are only positive and are with 50% ÷ 60% lower than the ones reported for the windward girders. And if they are used for design of the stabilizing elements of the girders, it would be in the direction of uncertainty;

e) in addition to forces in their plane, horizontal wind flows also cause forces in the vertical direction. Which forces in narrow bridges are unloading, but in wide ones, they are superimposed with gravitational loads.

From the conducted study of bridges with a vehicle on them, the following conclusions can be drawn:

a) in the general case, the conclusions stated above for bridges without a vehicle on them, are repeated;

b) the wind load on the windward girders is less, compared to the bridges without vehicles on them. On leeward girders practically no difference whether there is a vehicle on the bridges or not;

c) the total load on the internal girders may be in a direction coinciding with or opposite to the wind flow.

REFERENCES

1. AS/NZS 1170.2:2011. Structural Design Actions. Part 2: Wind actions. Standards Australia Limited / Standards New Zealand. ISBN 978-0-7337-9805-4.

2. BS 5400-2:2006. Steel, Concrete and Composite Bridges – Part 2: Specifications for Loads. British Standards Institution, 2006.

3. EN 1991-1-4:2005+A1:2010. Eurocode 1: Actions on structures – Part 1-4: General actions – Wind actions. European Committee for Standardization, Brussels, 2010.

4. IRC: 6-2017. Standard Specifications and Code of Practice for Road Bridges. Section: II – Loads and Load Combinations (Seventh Revision). Indian Road Congress, 2017.

5. Standards for Design of Road and Railway Bridges and Culverts. КТСУ, Sofia, 1989.

6. СП 35.13330.2011. Bridges and culverts. Ministry of Regional Development, Russian Federation, Moscow, 2011.

7. ANSYS® v.2020 R2. Documentation. Ansys Inc., Canonsburg, PA, the USA, 2020.

8. *Rusev, I., Tanev, T., Dinev, D*. Numerical study of wind actions on tall buildings with ANSYS CFX and comparison with EN1991-1-4. XII International scientific conference VSU'2012, Sofia, vol. 1, pp. 83-88, 2012. (on Bulgarian).

9. *Tominaga, Y., Mochida, A., Yoshie, R., Kataoka, H., Nozu, T., Yoshikawa, M., Shirasawa, T.* AIJ guidelines for practical applications of CFD to pedestrian wind environment around buildings. // Journal of Wind Engineering and Industrial Aerodynamics, 2008, 96 (10-11): 1749-1761. DOI: 10.1016/j.jweia.2008.02.058

10. *Rusev, I., Dinev, D., Tanev, T.* Numerical study of wind actions on nearby tall buildings. International Jubilee Scientific Conference UACEG'2012, Sofia, pp. 15-17, 2012. (on Bulgarian).

11. *Agyropulos, C., Markatos, N.* Recent advances on the numerical modelling of turbulent flows. // Applied Mathematical Modeling, 2015, 39: 693–732. DOI: http://dx.doi.org/10.1016/j.apm.2014.07.001.

12. *Markatos, N.* The mathematical modelling of turbulent flows. // Applied Mathematical Modeling, 1986, 10 (3): 190 - 220. DOI: https://doi.org/10.1016/0307-904X(86)90045-4

13. *Launder, B., Sharma, B.* Application of the energy dissipation model of turbulence to the calculation of flow near a spinning disk. Letters in Heat and Mass Transfer, 1974, 1, pp. 131–138.

14. *Baklanov, A., Barmpas, P., Bartzis, J., Batchvarova, E. et al.* Best practice guideline for the CFD simulation of flows in the urban environment. COST Action 732, Brussels, Belgium, 2007.

15. *Yu, M., Liao, H., Li, M., Ma, C., Luo, N., Liu, M.* Study on Static Wind Loading Coefficients of Suspension Bridge, Based on CFD Simulation and Wind Tunnel Test. // Applied Mechanics and Materials, 2011, 66-68: 334-339, Switzerland. DOI: http://dx.doi.org/10.4028/www.scientific.net/AMM.66-68.334

16. *Wassef, W.* Proposed Guide Specifications for Wind Loads on Bridges during Construction. AASHTO SCOBS T5 Meeting, Minneapolis, Minnesota. AECOM, 2016.

17. *Zdravkov, L.* Wind Loads on Girder Bridges. // Challenge Journal of Structural Mechanics, 2022, 8 (1): 9-16. DOI: https://doi.org/10.20528/cjsmec.2022.01.002